A novel method for measuring the bending rigidity of model lipid membranes by simulating tethers

Vagelis A. Harmandaris[a] and Markus Deserno[b]
Max-Planck-Institut für Polymerforschung, Ackermannweg 10, 55128 Mainz, Germany

(Received 24 August 2006; accepted 2 October 2006; published online 27 November 2006)

The tensile force along a cylindrical lipid bilayer tube is proportional to the membrane's bending modulus and inversely proportional to the tube radius. We show that this relation, which is experimentally exploited to measure bending rigidities, can be applied with even greater ease in computer simulations. Using a coarse-grained bilayer model we efficiently obtain bending rigidities that compare very well with complementary measurements based on an analysis of thermal undulation modes. We furthermore illustrate that no deviations from simple quadratic continuum theory occur up to a radius of curvature comparable to the bilayer thickness. © *2006 American Institute of Physics*. [DOI: 10.1063/1.2372761]

INTRODUCTION

Bilayer-forming lipids are the basic structural component of biological cell membranes. In these amphiphilic molecules a hydrophilic group is connected to one or two hydrophobic hydrocarbon chains. When dissolved into water they spontaneously assemble into a variety of structures. In nature lipid bilayers form the outer plasma membrane of cells as well as the walls of the different cellular compartments and organelles, such as the endoplasmic reticulum, the Golgi apparatus, and the nucleus.[1]

Lipid bilayer membranes display interesting physics on many different length and time scales. On atomistic length scales this includes questions such as how do lipid tail length and its degree of saturation influence the bilayer state, how does a specific hydrophilic head group facilitate solubilization, or how can water permeate the hydrophobic region? On somewhat larger scales the embedding of transmembrane proteins or bilayer fusion is being studied. And on scales exceeding several times the bilayer thickness, one may ask how vesicles are formed and what shape they have, which forces go along with a particular bilayer geometry, or how the demixing of a multicomponent membrane can trigger morphology changes. These different sets of questions require different techniques for their treatment. In the present article we focus on the physics happening on the large scale end, i.e., on the continuum level that may be employed on length scales beyond a few tens of nanometers, when a membrane may be viewed as a two-dimensional fluid elastic sheet.

As is typical in any coarse-graining scheme, many details pertaining to a physical system on a given scale get condensed into a few effective parameters on a larger level. Indeed, on the continuum level what remains of all lipid details are three material parameters: two moduli describing the softest deformation, which is bending, and one length scale describing a spontaneous curvature. The respective Hamiltonian, proposed in the early 1970s (Refs. 2–4) can be written as a surface integral over the entire membrane:

$$E = \int dA \left\{ \tfrac{1}{2}\kappa (K - C_0)^2 + \bar{\kappa} K_G \right\}. \tag{1}$$

Here, the extrinsic curvature $K = 1/R_1 + 1/R_2$ is the sum of the two local principal curvatures, and the Gaussian curvature $K_G = 1/(R_1 R_2)$ is their product. The inverse length C_0 indicates any spontaneous curvature which the bilayer might have, so the first term quadratically penalizes deviations of the local extrinsic curvature from C_0. The two moduli κ and $\bar{\kappa}$ belonging to the two quadratic curvature expressions are referred to as *bending modulus* and *saddle splay modulus*, respectively. If the membrane has two identical leaflets, $C_0 = 0$ by symmetry, a situation which does seldomly hold for biological membranes but very frequently for artificial lipid bilayers and vesicles. Furthermore, since the surface integral over the Gaussian curvature K_G can be expressed as a boundary integral plus a topological term, the second term in Eq. (1) most often only contributes a constant and can then be ignored. Under these conditions there remains only a single physical parameter characterizing the membrane, the bending modulus κ, and it is thus the most important one to determine.

Bending rigidities have been measured experimentally by various techniques,[5–15] all ultimately based on one of two general approaches: One may either utilize the dependence of thermal undulations on a membrane's rigidity or measure the force needed to actively bend it. The traditional realization of the first approach is to monitor the fluctuations of vesicles as a function of wavelength by light microscopy, a method termed "flicker spectroscopy."[5–7] A related experimental method is based on micropipette manipulation techniques. There, the flicker spectrum is successively suppressed by increasing the pipette pressure, and the bending rigidity can then be obtained from the low-tension regime of the tension-area curve.[8–11] The second approach is typically implemented by measuring the force needed to pull nanoscale bilayer tubes (tethers) from vesicles.[12–15] Since the for-

[a]Electronic mail: harmanda@mpip-mainz.mpg.de
[b]Electronic mail: deserno@mpip-mainz.mpg.de

mation of a tube involves the creation of a high curvature, the work to pull a tether is basically done against bending energy; hence the modulus κ can be determined from it.

Determination of the bending rigidity is of course equally important in computer simulation studies of lipid bilayers, and the spectrum of available methods is the same. However, by far the most common approach in simulations is flicker spectroscopy, both for atomistic simulations[16–18] as well as for various coarse-grained methods.[18–24] Only recently den Otter and Briels have proposed a method by which constraining forces are applied to actively deform the membrane,[25] and Farago and Pincus have proposed a scheme based on the change in free energy of deforming the bilayer.[26] Unfortunately, both active methods involve significant technical and conceptual sophistication. This may explain why the idea is not commonly employed, despite the fact that particularly for stiff membranes fluctuation based schemes encounter difficulties (in experiments as well as in simulations), because the thermally excited amplitudes decrease with bending modulus and become difficult to resolve at some point.

In the present article we propose an alternative simulation approach for studying the curvature elasticity of membranes by an active deformation. Our setup essentially involves measuring the force necessary to hold a membrane tether, and it is thus conceptually identical to its experimental "counterpart." As we will see, complications of earlier active schemes are avoided, and the simulations are very easy to perform and analyze. We apply this method to a recently proposed coarse-grained solvent-free simulation model[22,23] and find results that agree very well with data from the analysis of the thermal fluctuations. Moreover, the method permits us to check, up to which curvatures the quadratic model from Eq. (1) remains valid. Our results indicate that curvature radii close to the bilayer thickness can be imposed without noticeable deviations from Eq. (1). While the precise location for the breakdown of quadratic theory may well be model dependent, its validity up to length scales comparable to bilayer thickness is in agreement with experimental findings.[15]

CURVATURE ELASTICITY

In this section we first briefly review the fluctuation approach towards bilayer elasticity and discuss some of its difficulties. We then introduce the alternative scheme based on holding a membrane tether.

Flicker spectroscopy

The energy expression in Eq. (1) requires knowledge of the local membrane curvature. For essentially flat membranes, which can be described by specifying their height $h(x,y)$ above some reference plane ("Monge parametrization"), this curvature is given by

$$K = \nabla \cdot \left(\frac{\nabla h}{\sqrt{1 + (\nabla h)^2}} \right) \overset{|\nabla h| \ll 1}{\approx} \Delta h, \tag{2}$$

where ∇ is the two-dimensional nabla operator on the base plane. The approximation in the second step is the lowest order term in a small gradient expansion. On this level the Hamiltonian (1) becomes quadratic and can be diagonalized by Fourier transformation. Assuming an $L \times L$ membrane patch with periodic boundary conditions and writing $h(\boldsymbol{r}) = \Sigma_{\boldsymbol{q}} h_{\boldsymbol{q}} e^{i\boldsymbol{q}\cdot\boldsymbol{r}}$, one finds

$$E = \tfrac{1}{2} L^2 \sum_{\boldsymbol{q}} |h_{\boldsymbol{q}}|^2 (\kappa q^4 + \Sigma q^2), \tag{3}$$

where we for completeness also added a surface tension term Σ times excess area. From the equipartition theorem we then see that the mean squared amplitude of each mode, i.e., the *fluctuation spectrum* or the *static structure factor*, is given by

$$\langle |h_{\boldsymbol{q}}|^2 \rangle = \frac{k_B T}{L^2 (\kappa q^4 + \Sigma q^2)}. \tag{4}$$

A fit of the fluctuation spectrum measured in the simulation to this expression yields bending modulus κ and tension Σ. Since for wave vectors smaller than $q_{\min} \simeq \sqrt{\Sigma/\kappa}$ the fluctuations are tension dominated, it is best to simulate at zero tension in order to avoid unnecessary damping of the most relevant modes. In this case the expression $1/(q^4 \langle |h_{\boldsymbol{q}}|^2 \rangle L^2)$ approaches $\kappa/k_B T$ in the limit $q \to 0$, as is illustrated in Fig. 1 for a model simulation[22,23] described in more detail below. For wave vectors approaching $q_{\max} \simeq 2\pi/w$, where w is the bilayer thickness, discrete lipid fluctuations such as protrusions require a more careful analysis.[24]

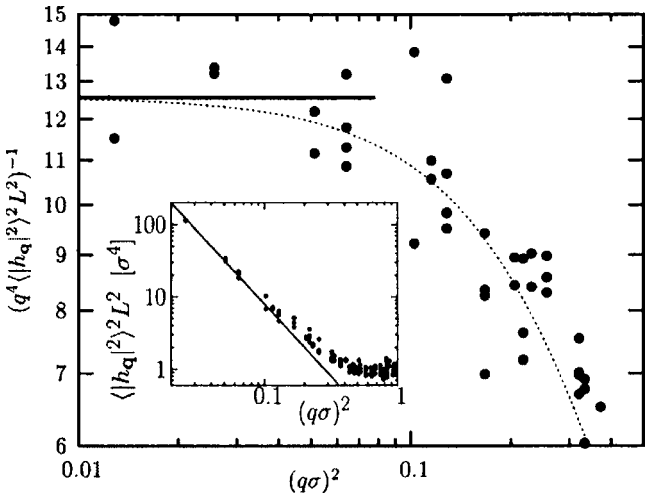

FIG. 1. Flicker spectrum of a fluctuating membrane, plotted in such a way that in the limit $q \to 0$ the expression approaches κ, see Eq. (4). The dashed line is a fit of the form $(k_B T/\kappa + c_1 (q\sigma)^{c_2})^{-1}$ which helps to find the asymptotic value; the inset shows the unscaled spectrum. The fit leads to $\kappa = 12.5 k_B T$, with an error estimated to be $\pm 1 k_B T$. The system is the same lipid bilayer model (Refs. 22 and 23) that will be used for the tethers, see below.

There are clear limitations for the calculation of κ using thermal fluctuations. The first and obvious one is that large values of κ lead to very small amplitudes. Considering (i) that $\kappa/k_B T$ is typically of order 10 and (ii) how strongly the amplitudes decay with increasing wave vector, one realizes that it requires substantial statistics to be able to resolve the spectrum. Particularly unpleasant in this context is that the most important low-q modes equilibrate slowest, with a time scale diverging like q^{-4}.

Also, it must be appreciated that the curvatures *probed*

this way are very weak. Since (in the tensionless state) $\langle K^2\rangle = q^4\langle|h_{\mathbf{q}}^2|\rangle = k_BT/L^2\kappa$, the average (root-mean-square) radius of curvature is given by $\bar{R}=\langle K^2\rangle^{-1/2}=L\sqrt{\kappa/k_BT}$, i.e., several times the box length. These curvatures are *much* weaker than the ones which one usually imposes on systems if one studies vesicles, budding, tubes, or fusion. This leaves the question open how *relevant* the measured elastic constants really are.

It is also these limitations which den Otter and Briels[25] had in mind when they proposed ways for obtaining larger curvatures, either by more advanced sampling techniques, such as umbrella sampling, or by explicitly creating undulations with larger amplitudes by suitable constraints. They found that for larger amplitudes the membrane seemed to stiffen, which might suggest that the simple curvature elastic model underlying Eq. (1) breaks down. However, an alternative explanation would be provided by the neglect of higher order terms in the small gradient approximation for the curvature in Eq. (2). Indeed, for a mode $h(x,y)=a\sin(qx)$, it is easy to verify that the ratio between linear and nonlinear predictions of the curvature energy is given by

$$\frac{E_{\mathrm{lin}}}{E_{\mathrm{nonlin}}} \overset{qa\gg 1}{=} \frac{3\pi}{8}qa + \frac{3\pi}{32}(qa)^{-1} + \mathcal{O}((qa)^{-3}), \tag{5}$$

which diverges linearly with growing amplitude. While this is qualitative what den Otter and Briels observe, the magnitude of their stiffening is bigger than what Eq. (5) would predict. The observed deviation for large amplitudes appears more likely to be a result of a residual tension stemming from their simulations being done at constant box volume.

Stretching tethers

Here we present a method for the calculation of κ based on a different approach. The basic idea is to impose a deformation of the membrane, specifically by creating a curved cylindrical vesicle, and then measure the force required to hold it in this deformed state. In the experiment such tethers are typically created by first attaching adhesive beads to a suitably fixated giant vesicle (or a cell) and then pulling it away with a laser tweezer that permits the measurement of the involved force. In the simulation such a tether can simply be stabilized by "spanning" a cylindrical vesicle through the simulation box, *across* the periodic boundary conditions. One thus simulates a system which is perfectly cylindrical (i.e., there are no end effects), and the axial pulling force is readily obtained from the component of the stress tensor along the box-spanning direction.

With a vesicle radius R and a box length L_z in the direction of the spanned vesicle, see Fig. 2, the curvature energy is

$$E = \frac{\kappa}{2}\left(\frac{1}{R}\right)^2 2\pi R L_z = \frac{\pi\kappa L_z}{R}. \tag{6}$$

The axial force under the constraint of fixed area $A=2\pi RL_z$ is obtained from $F_z=(\partial E/\partial L_z)_A=2\pi\kappa/R$; hence the bending modulus is given by

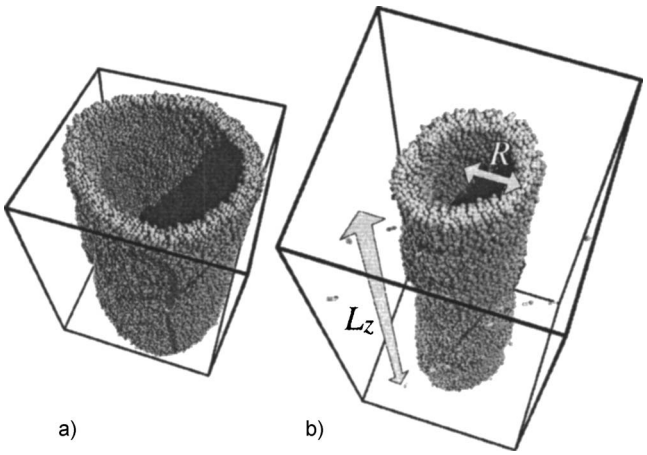

FIG. 2. Snapshots of two tether simulations with 20 000 lipids and different radii of curvature: (a) $\langle R\rangle=24\sigma$ and (b) $\langle R\rangle=12\sigma$.

$$\kappa = \frac{F_z R}{2\pi}. \tag{7}$$

Since both F_z and R are easily measurable, κ can be readily determined in the simulation. In fact, it is this point where implementing the tether method in a simulation shows its biggest advantage over its experimental counterpart: In a real experiment R cannot be measured directly, since its typical magnitude is suboptical. It is thus usually reexpressed in terms of the membrane tension Σ, leading to $R=\sqrt{\kappa/2\Sigma}$ and thus $\kappa=(F_z/2\pi)^2/2\Sigma$, but then the tension needs to be monitored independently by other means. Recently, however, Cuvelier *et al.*[15] devised a clever setup involving *two* tethers which avoids such complications.

Even though the above analysis is standard in the tether literature,[12–15] it is still only approximate. Notice that this time we have neglected thermal fluctuations altogether. The formula (7) relies entirely on a "ground state" argument. This is justifiable in two ways. First, for not too small radii of curvature, the fluctuation contribution to the force, as estimated for instance by a simple plane-wave ansatz for the cylindrical modes, turns out to be very small. And second, the two most obvious effects which fluctuations have on the two terms in Eq. (7) that need to be determined, F_z and R, are working in opposite directions. While clearly the mean axial force $\langle F_z\rangle$ will increase (for exactly the same reason that it takes a force to pull a fluctuating polymer straight), the fluctuation-corrected mean radius $\langle R\rangle$ of the vesicle will decrease, since the total area is constant and the area needed for fluctuations has to come from somewhere. Within a plane-wave approximation these two effects cancel. A more accurate investigation is a fair bit more subtle.[27]

By performing various simulations of tethers with different curvature radii R, we can thus address the question how far the present quadratic theory remains valid. Assuming symmetric membranes, the next terms by which the Hamiltonian density in Eq. (1) needs to be amended are quartic ones, and these are K^4, K^2K_G, K_G^2, and the gradient term $(\nabla_a K)(\nabla^a K)$, where ∇_a is the metric-compatible covariant derivative.[28] Since for cylinders $K_G=0$ and $|\nabla_a K|=0$, the

TABLE I. List of all simulation geometries, sorted by the number of lipids (first column) and their tether length (in units of σ, first row). In all tuples the top value indicates $\langle R\rangle$ (in units of σ), and the bottom value is $\langle F_z\rangle$ (in units of ϵ/σ). We always used $w_c=1.6\sigma$ and $k_BT=1.1\epsilon$.

No. of lipids	$L_z=20$	30	40	50	60	70	80	90	100	120	160	200	240
5000	24.0±0.5 3.96±0.9	16.1±0.4 5.4±0.8	12.2±0.3 6.12±0.8	9.8±0.2 8.28±0.8	8.3±0.2 10.44±0.8	7.2±0.1 11.52±0.8	6.3±0.1 12.6±0.8	5.7±0.1 13.68±0.8	⋯	⋯	⋯	⋯	⋯
10 000	47.8±0.6 1.8±0.7	⋯	24.0±0.4 3.24±0.7	⋯	16.0±0.4 4.68±0.8	⋯	12.2±0.2 6.8±0.8	⋯	9.9±0.2 8.28±0.8	8.3±0.1 10.5±0.7	6.3±0.1 12.5±0.8	⋯	⋯
20 000	⋯	⋯	47.7±0.6 1.7±0.8	⋯	⋯	⋯	24.0±0.4 3.5±0.8	⋯	⋯	16.0±0.3 4.7±0.8	12.1±0.2 6.6±0.8	9.9±0.2 8.3±0.8	8.3±0.1 10.4±0.8

only remaining term is K^4. Adding $\frac{1}{4}\kappa_4 K^4$ to the energy density and repeating the steps leading to Eq. (7), we then find

$$\frac{F_z R}{2\pi} = \kappa + \frac{\kappa_4}{R^2} = \kappa[1+(\ell_4 K)^2], \tag{8}$$

where $\ell_4=\sqrt{\kappa_4/\kappa}$ is a characteristic length scale associated with corrections beyond quadratic order, and one typically assumes that it is related to bilayer thickness.

MESOSCOPIC MEMBRANE SIMULATION

To illustrate our method, we have performed mesoscopic simulations of a coarse-grained lipid bilayer model recently developed in our group.[22] Roughly, lipids are represented by three consecutive beads of diameter σ (our unit length), with one end bead being hydrophilic and the two tail beads hydrophobic. The latter feature, in addition to an excluded volume interaction, an attraction with a tunable depth ϵ (our unit of energy) and range w_c. The unit of time is $\tau=\sigma\sqrt{m/\epsilon}$, where m is the unit of mass. By properly choosing w_c and ϵ, a wide range of self-assembling fluid bilayer phases of different bending rigidities is obtained. More details can be found in Refs. 22 and 23.

Coarse-grained molecular dynamics simulations of a lipid systems with $w_c=1.6\sigma$ and $k_BT=1.1\epsilon$ were performed using the ESPRESSO package.[29] The geometries studied are summarized in Table I. All simulations were performed under canonical (NVT) conditions, using a Langevin thermostat[30] with friction constant $\Gamma=1.0\tau^{-1}$ to keep the temperature constant. Within a rectangular box with dimensions $L_x=L_y$ and L_z, using periodic boundary conditions in all directions, a cylindrical membrane spanning the z direction was initially set up with a radius R_{setup} chosen in such a way that the area per lipid in both leaflets corresponded to the one for a flat tensionless bilayer.[23] Upon starting the simulation R_{setup} relaxed (typically within about 1000τ) to its equilibrium value $\langle R\rangle$, which is smaller than R_{setup} by about 3%–5% due to the area required for fluctuations. For this to happen it was quite advantageous that the flip-flop rate of lipids between the two leaflets is big enough to permit efficient relaxation of area-difference strains going along with changes of the mean radius. For the integration, a time step of $\Delta t=0.005\tau$ was used for most of the systems, while in some cases we needed a smaller time step of $\Delta t=0.001\tau$ in order to obtain accurate results.

RESULTS AND DISCUSSION

Figure 2 shows two typical snapshots of equilibrated cylindrical vesicles from different simulations. Notice that while fluctuations are clearly visible, they are fairly weak, i.e., the vesicle is to a very good approximation cylindrical. We use the midplane between the two monolayers to denote the average radius $\langle R\rangle$. It is determined by first identifying the axis and next finding the average distance of the second tail bead of the outer leaflet to this axis, R_{out}, and the equivalent for the inner leaflet, R_{in}. We then take $\langle R\rangle=\frac{1}{2}\langle R_{\text{out}}+R_{\text{in}}\rangle$, where the average is taken during long production runs typically extending over $10\,000-20\,000\tau$. Errors are determined via a blocking analysis. During these runs we also measure the stress tensor σ_{ij} using the virial theorem.[31] Figure 3 shows a typical example of the running average of the three normal stress components. As we observe, the axial stress σ_{zz} has a finite value. In contrast, σ_{xx} and σ_{yy} (as well as all off-diagonal components not shown here) approach zero. This is expected, since no stress is being transported across the x and y directions. The error in σ_{zz} is also determined via a blocking analysis.

One more point concerning the calculation of the stress tensor should be mentioned. In general, deriving accurately the stress (or the pressure) from molecular dynamics simulations is not a trivial aspect. Stress is a collective property with high statistical uncertainty owing to the fluctuations of

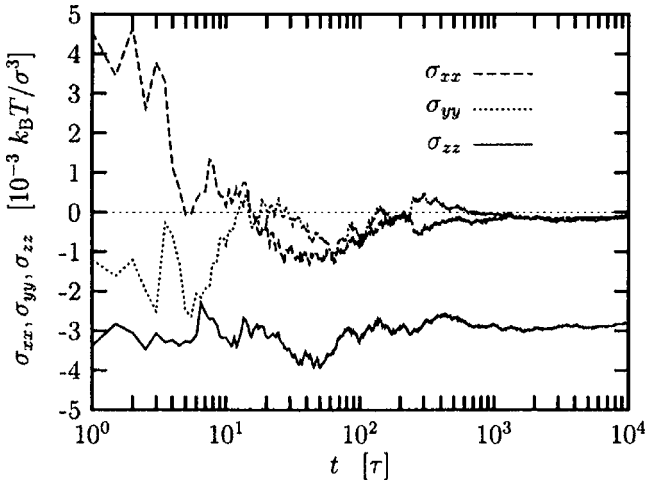

FIG. 3. Running average of the diagonal components σ_{xx}, σ_{yy}, and σ_{zz} of the stress tensor for a cylindrical vesicle with $\langle R\rangle=70\sigma$.

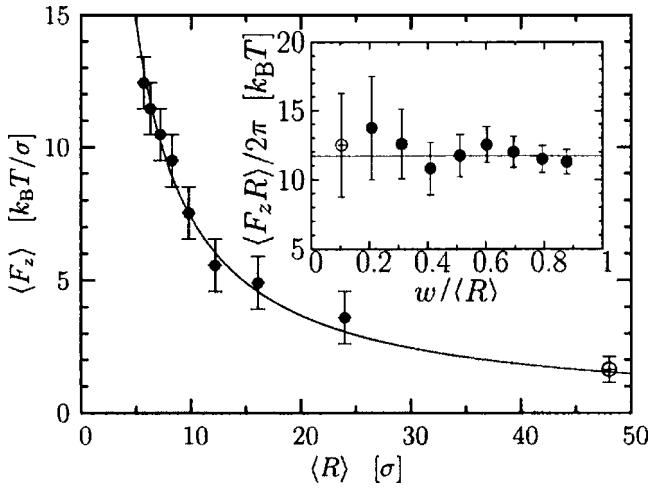

FIG. 4. Tensile force $\langle F_z \rangle$ as a function of cylinder radius $\langle R \rangle$ for the systems with $N=5000$ lipids (with the exception of the open symbol, which has $N=10\,000$ lipids). The solid line is a fit to Eq. (7), leading to $\kappa=11.7k_BT$. The inset shows the combination $F_zR/2\pi$ as a function of rescaled curvature $w/\langle R \rangle$, and the solid line again indicates $\kappa=11.7k_BT$.

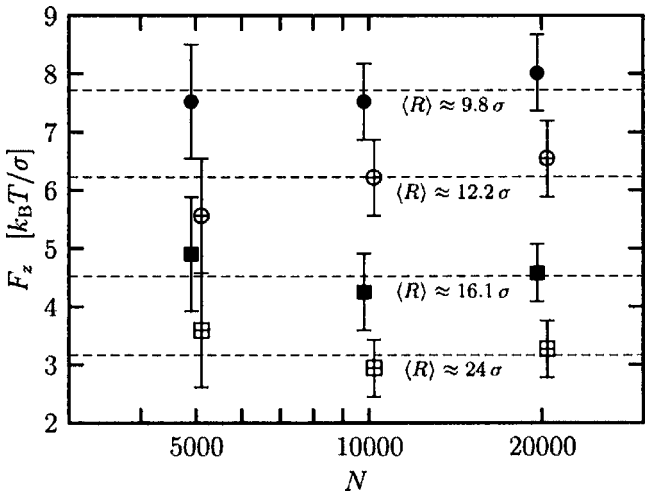

FIG. 5. Tensile force F_z as a function of system size for systems of different ratio L_z/N: (●) 0.01, (◯) 0.008, (■) 0.006, and (□) 0.004. The corresponding average radius $\langle R \rangle$ is also indicated. A slight horizontal offset is included to improve visibility of the error bars.

the instantaneous configurations. In common simulations these fluctuations are very high due to the relatively small size (number of particles) of the systems studied. Therefore large systems and/or long simulation runs are needed. This point is particularly severe in the present case since, as visible in Fig. 3, we need to determine very small values of the stress. We have found that, in order to obtain reliable values, the common time step used in coarse-grained simulations, $\Delta t=0.01\tau$, is too long. With this choice σ_{xx} and σ_{yy} approached values which were significantly different from zero, a clear sign of a systematic integration error. We thus used the smaller time step $\Delta t=0.005\tau$, and for the cases of very small forces, i.e., large $\langle R \rangle$, even a time step of $\Delta t=0.001\tau$.

The tensile force in the z direction is obtained from the stress via $F_z=\sigma_{zz}L_xL_y$. Figure 4 shows the force for the systems with $N=5000$ lipids as a function of the average cylinder radius $\langle R \rangle$. As the radius increases, the tensile force F_z decreases in accord with Eq. (7). This is seen even better by looking at the combination $F_zR/2\pi$, which is shown in the inset of Fig. 4 as a function of rescaled curvature $w/\langle R \rangle$. Notice that within the error bars of our simulation this expression is perfectly compatible with a constant; a fit gives $\kappa/k_BT=11.7\pm0.2$, in very good agreement with the value $\kappa/k_BT=12.5\pm1$ obtained from an analysis of thermal undulation modes (see Fig. 1). A possible quadratic deviation, as suggested by Eq. (8), cannot be identified with any statistical significance. This is all the more amazing when we see that the most strongly curved cylinder has $w/R\approx0.9$, i.e., a radius of curvature which is only 10% larger than the bilayer thickness w. Stated differently, the length ℓ_4 from Eq. (8) must be a fair bit smaller than w. This remarkable robustness of the simple quadratic Helfrich theory down to such small radii of curvature might of course be a special feature of the particular model we have studied, and it would be worthwhile to subject other coarse-grained lipid models to a similar test. But the fact that extremely high curvatures can be imposed without noticing deviations from quadratic continuum theory is in accord with common practice in tether pulling experiments, where the radii of curvature of these membrane tubes are typically in the 10–40 nm range, apparently without ever having triggered the need to include higher order corrections to the elastic behavior.[15]

Another practical aspect of our proposed method is related to numerical efficiency. The traditional method of analyzing the thermal fluctuation spectrum requires very long simulation runs, since (i) large systems need to be studied in order to have a series of wave vectors in the regime where continuum methods are applicable and (ii) these long wavelength modes take a particularly long time to equilibrate (the relaxation time of bending modes scales with the fourth power of wavelength). Strictly speaking our method also requires large systems to be studied in order to extrapolate to the zero curvature limit (i.e., $R\to\infty$). However, as we have seen in Fig. 4, the asymptotic limit in our case is already reached for fairly small systems which still have a significant curvature. If the same holds for other lipid models—a fact that needs to be checked—their value of κ can also be determined via the tether method using fairly small systems and corresponding small simulation times. For example, the point in Fig. 4 having $w/\langle R \rangle=0.5$ is taken from a run of only 2–3 days on a single AMD Opteron 2.2 GHz processor. For the same system the analysis of the thermal fluctuations needs at least 1 month on the same machine.

As a final point we would like to address the issue of finite size effects. While the tether force obviously depends on its radius, Eq. (7) suggests that tether *length* L_z (or equivalently, the number N of lipids) is irrelevant. This is indeed rigorously true in the ground state, but fluctuations might change the picture. We have thus repeated our simulations for systems with a different number of lipids and checked whether systems with a fixed ratio L_z/N (i.e., essentially identical radius) but varying N show any noticeable systematic change in the tensile force F_z. Figure 5 shows the results of such simulations. As can be seen, the measured forces are, at least within our error bars, compatible with a

constant value for a fixed ratio L_z/N. No finite size effect is detectable. Notice that this also provides another independent check that fluctuations in our system, even though present, are a subdominant effect compared to the main "signal" which is well described by ground state theory.

CONCLUSIONS

We have presented a new method for calculating the bending rigidity of lipid membranes in simulations. It involves the simulation of cylindrical membrane tethers, spanned across the periodic boundary conditions of the simulation box, and measuring their equilibrium radius as well as the tensile force they exercise on the box. In contrast to fluctuation based schemes, which monitor thermally excited shape deformations, our approach actively imposes a deformation on the system and measures the restoring force and is thus not limited to the regime of deformations accessible by thermal energy. In fact, thermal undulations only contribute a small correction to the main observable, in stark contrast to fluctuation schemes in which they provide the dominant signal. For this reason our method is very efficient, also applicable to stiff membranes which show very small undulations to begin with, and does not crucially depend on the relaxation of very slow long wavelength modes. The straightforward access to strong bending permits a check of quadratic continuum theory, without running into difficulties of Monge gauge and its linearization. For the coarse-grained lipid model we explicitly studied, we showed continuum theory to be applicable up to curvatures comparable to bilayer thickness. Finite size effects would originate from fluctuations and are thus also weak; in our runs they were not detectable.

We believe that this method provides a powerful alternative to the existing schemes that is worth to be applied to other existing coarse-grained models. Not only is an independent measurement of the elastic modulus very valuable, determining the range of validity of continuum theory for each model would be an important bit of knowledge, given that the curvatures that are regularly imposed in simulations exceed thermally excited ones by at least one or two orders of magnitude.

ACKNOWLEDGMENTS

We are grateful to I. Cooke for his help with the coarse-grained simulations and to J.-B. Fournier, W. den Otter, W. Briels, B. Reynolds, N. van der Vegt, and K. Kremer for useful discussions. One of the authors (M.D.) acknowledges financial support by the German Science Foundation under Grant No. De775/1–3.

[1] H. Lodish, A. Berk, L. Zirpursky, P. Matsurada, D. Baltimore, and J. Darnell, *Molecular Cell Biology* (Freeman, New York, 2000).
[2] P. B. Canham, J. Theor. Biol. **26**, 61 (1970).
[3] W. Helfrich, Z. Naturforsch [C] **28**, 693 (1973).
[4] E. Evans, Biophys. J. **14**, 923 (1974).
[5] F. Brochard and J. F. Lennon, J. Phys. (Paris) **36**, 1035 (1975).
[6] M. D. Schneider, J. T. Jenkins, and W. W. Webb, J. Phys. (Paris) **45**, 1457 (1984).
[7] J. F. Faucon, M. D. Mitov, P. Meleard, I. Bivas, and P. Bothorel, J. Phys. (Paris) **50**, 2389 (1989).
[8] E. Evans and W. Rawicz, Phys. Rev. Lett. **64**, 2094 (1990).
[9] W. Rawicz, K. C. Olbrich, T. McIntosh, D. Needham, and E. Evans, Biophys. J. **79**, 328 (2000).
[10] J. R. Henriksen and J. H. Ipsen, Eur. Phys. J. E **9**, 365 (2002).
[11] J. R. Henriksen and J. H. Ipsen, Eur. Phys. J. E **14**, 149 (2004).
[12] L. Bo and R. E. Waugh, Biophys. J. **55**, 509 (1989).
[13] J. Dai and M. P. Sheetz, Biophys. J. **68**, 988 (1995).
[14] E. Evans, H. Bownman, A. Leung, D. Needham, and D. Tirrell, Science **273**, 933 (1996).
[15] D. Cuvelier, I. Derenyi, P. Bassereau, and P. Nassoy, Biophys. J. **88**, 2714 (2005).
[16] E. Lindahl and O. Edholm, Biophys. J. **79**, 426 (2000).
[17] S. J. Marrink and A. E. Mark, J. Phys. Chem. B **105**, 6122 (2001).
[18] E. D. Boek, J. T. Padding, W. K. den Otter, and W. J. Briels, J. Phys. Chem. B **109**, 19851 (2005).
[19] R. Goetz, G. Gompper, and R. Lipowsky, Phys. Rev. Lett. **82**, 221 (1999).
[20] O. Farago, J. Chem. Phys. **119**, 596 (2003).
[21] M. J. Stevens, J. Chem. Phys. **121**, 11942 (2004).
[22] I. R. Cooke, M. Deserno, and K. Kremer, Phys. Rev. E **72**, 011506 (2005).
[23] I. R. Cooke and M. Deserno, J. Chem. Phys. **123**, 224710 (2005).
[24] G. Brannigan and F. L. H. Brown, Biophys. J. **90**, 1501 (2006).
[25] W. K. den Otter and W. J. Briels, J. Chem. Phys. **118**, 4712 (2003).
[26] O. Farago and P. Pincus, J. Chem. Phys. **120**, 2934 (2004).
[27] J.-B. Fournier and P. Galatola (unpublished).
[28] R. Capovilla, J. Guven, and J. A. Santiago, J. Phys. A **36**, 6281 (2003).
[29] H. J. Limbach, A. Arnold, B. A. Mann, and C. Holm, Comput. Phys. Commun. **174**, 704 (2006); http://www.espresso.mpg.de/
[30] G. S. Grest and K. Kremer, Phys. Rev. A **33**, 3628 (1986).
[31] M. P. Allen and D. J. Tildesley, *Computer Simulation of Liquids* (Clarendon, Oxford, 1997).